



3 1176 00073 0565

TECHNICAL MEMORANDUMS

NATIONAL ADVISORY COMMITTEE FOR AERONAUTICS

No. 721

RESULTS OF EXTENDED TESTS OF THE
FOCKE-WULF F 19a "ENTE", A TAIL-FIRST AIRPLANE

By Walter Hübner

Zeitschrift für Flugtechnik und Motorluftschiffahrt
Vol. 24, Nos. 8 & 9, April 28, and May 13, 1933
Verlag von R. Oldenbourg, München und Berlin

Washington
September 1933

1.7.1.2
1.7.1.3
1.8.5
1.8

NATIONAL ADVISORY COMMITTEE FOR AERONAUTICS

TECHNICAL MEMORANDUM NO. 721

RESULTS OF EXTENDED TESTS OF THE

FOCKE-WULF F 19a "ENTE", A TAIL-FIRST AIRPLANE*

By Walter Hübner

Measurements were made for the determination of the characteristics of tail-first airplanes in general and of the Focke-Wulf F 19a "Ente" in particular. These investigations consisted chiefly of measurements of the take-off distance under various starting conditions and with the c.g. in different positions; of the climbing speed as a function of the impact pressure and location of the c.g.; of the static longitudinal stability and fore-and-aft controllability and of the determination of the elevator forces and characteristics of the elevator control. General observations of the airplane were made, especially in flight at large angles of attack and in squally weather, for the determination of safety in operation. These measurements are part of an extensive program of investigation for the determination of the characteristics of tail-first airplanes.

I. REASON FOR INVESTIGATION

Several tail-first types were known before the war. They were subsequently discarded for various reasons none of which, however, was the fault of the design. After the war tail-first gliders were built and tested by Klemperer and Lippisch (Rhön-Rossitten-Gesellschaft). The experience gained was not, however, applied to the construction of powered airplanes. A twin-engine tail-first airplane was built in 1926-27 by the Focke-Wulf Company, Bremen, on the basis of tests made in 1907. This airplane was destroyed in 1927 in a crash for which the tail-first design cannot

*"Einige Ergebnisse der erweiterten Prüfung der Eigenschaften des Flugzeugs Focke-Wulf F 19a "Ente". Zeitschrift für Flugtechnik und Motorluftschiffahrt, April 28, 1933, pp. 223-230; and May 13, 1933, pp. 255-258.

be held responsible. A second airplane was built in 1930. The probable cause of the above crash was remedied in this new type by slight modifications. This example met entirely the requirements for transport airplanes. After passing the type test it was put in service on commercial passenger lines. A series of measurements for the determination of the characteristics of tail-first airplanes was made with this type, known as the F 19a. The main results are given below.

II. OBJECT OF TESTS

Incorporation of the best performance features and weight characteristics in the design of the F 19a was intentionally avoided. The main task was rather to adapt the flight characteristics to the needs and requirements of the moment. Hence, the purpose of the present investigation is not to compare the performances of the "Ente" with those of standard types, but merely to determine its characteristics. During the tests it was found necessary to incorporate in the program the determination of the performances with the c.g. in different positions. Thus extended, the problem covered the following subjects:

Determination of take-off distance under different conditions and with the c.g. in various positions;

Determination of climbing speed at full throttle and with the c.g. in different positions;

Determination of fore-and-aft stability with locked controls at full throttle.

Measurement of elevator stresses with different locations of the c.g. and determination of the controllability.

Study of flight under various weather conditions.

The results of the above measurements are given below. Another series of tests is contemplated, especially for the determination of directional stability and its relation to the size of the lateral fins under the wing, and for a dynamic study of the airplane at large angles of attack.

III. NOTATION

- c_a = lift coefficient of airplane for total wing area.
 c_w = drag coefficient for total wing area.
 c_{mH} = moment coefficient of airplane about transverse axis.
 c_{RH} = elevator moment coefficient.
 α = angle of attack in degrees = angle between propeller axis and flight path (positive when airplane noses up).
 α_H = angle of attack of stabilizer in degrees = angle between stabilizer chord and flight path (positive when airplane noses up).
 θ = fore-and-aft inclination in degrees = angle between propeller axis and horizon (positive when airplane noses up).
 ϕ = climbing angle in degrees = angle between flight path and horizon (positive when climbing).
 β_H = elevator deflection in degrees (positive when stick is pulled back).
 β_{H_s} = control-stick deflection in degrees (positive when stick is pulled back).
 k = control gear ratio β_{H_s}/β_H .
 η = propeller efficiency
 λ = coefficient of propeller advance.
 r = rearward position of c.g. in percent of t_m (positive toward rear) (fig. 1).
 b = span of main wing in meters.
 t_m = mean wing chord in meters = wing chord at $2b/3\pi$ from center of wing = 2.5 m (8.2 ft.).
 t_{HR} = elevator chord in meters.

- e_H = length of elevator control lever in meters.
- S = ground run in meters.
- G = total or gross weight in kg.
- P = manual force in kg on control stick (positive with nose-heavy airplane) (fig. 24).
- P_G = control force on stick in kg = force required to balance moment of control weight (positive when airplane is nose-heavy) (fig. 24).
- P_L = force of elevator moment on control stick = force required to balance moments produced by air forces about elevator axis (positive with nose-heavy airplane) (fig. 24).
- P_R = friction force on control stick in kg = force required to overcome friction of control.
- t = time in seconds.
- F = total wing area in m^2 = area of main wing + area of forward wing = $35.7 m^2$ (384 sq.ft.).
- F_H = area of forward wing in m^2 $6.2 m^2$ (67 sq.ft.).
- F_{HR} = elevator area in m^2 = $1.7 m^2$ (18.3 sq.ft.).
- v = flying speed in m/sec.
- v_{st} = climbing speed in m/sec.
- n = propeller r.p.m.
- M_H = moment about transverse axis in m-kg.
- N = engine power in hp.
- q = dynamic pressure in kg/m^2 .
- γ = specific gravity of air in kg/m^3 .
- g = acceleration due to gravity = $9.81 m/sec^2$.

IV. TEST PROCEDURE

1. Instruments and Calibration

The dynamic pressure is measured with an Askania dynamic pressure recorder calibrated in flight; the altitude, with an Askania barograph; the fore-and-aft inclination, with a DVL inclinometer integral with the barograph; the elevator deflection, with a DVL deflection recorder; and the stick force, with a DVL stick-force recorder. The instruments are simultaneously switched on and off by an electric switch on the stick-force recorder. The revolution speed is measured with the standard airplane revolution counter. The take-off distance is recorded with the DVL take-off recording camera. A thin layer of snow covered the ground on the day of the take-off tests. The take-off run was thus directly shown by the marks of the front and rear wheels of the airplane. The ground wind was measured with a Fuess anemometer.

2. Preliminary Measurements

In flight, the elevator moments produced by the air forces and the moments of the control weights are balanced by the pilot. In accelerated flight the control friction, the air force moments, and the control moments have to be overcome. The moments of the control weights, for which allowance must be made in the interpretation, are measured at various fore-and-aft inclinations (fig. 2). The force applicable by the pilot on the control stick depends on the gear ratio of the controls. This gear ratio was measured (fig. 3).

Two Heine propellers with a diameter of 2.45 m and a pitch of 2.11 m were used in the test flights. The propellers were calibrated in a flight with wide-open throttle at 100 to 200 m height (fig. 4).

The position of the c.g. and the total weight were determined in each load case by weighing twice on three scales placed under the landing-gear wheels.

3. Flight Measurements

a) Effect of elevator deflection on take-off distance.- In various tests the direction and magnitude of the elevator deflection were found to affect materially the length of the take-off run. By pushing the elevator control at the start the take-off run was not reduced but increased. Hence an attempt was made to determine the numerical value of the influence of the elevator setting on the length of the take-off run.

Three take-off measurements were made for this purpose on the same day, in the same place, under the same general conditions and in perfectly quiet weather. The airplane took off from a concrete runway covered with a thin layer of fresh snow. Before each start the airplane was brought to the same starting point where the ground was sanded to enable the wheel brakes to take effect. The engine was started with brakes applied. The latter were released after reaching full engine power. In the first test the elevator was immediately deflected through -12.5° . As soon as the airplane acquired the necessary speed, the front wheel and then the whole airplane were taken off by pulling the elevator control. The same procedure was adopted for the second and third tests with initial elevator deflections of -3.5° and $+0.8^{\circ}$ respectively.

b) Determination of the influence of the location of the c.g. on the take-off run.- Measurements with the c.g. in three different positions were made under the best conditions for shortening the take-off run. The total airplane weight was 1500 kg (3307 lb.). The position of the c.g. was changed by ballast weights carried in the fuselage. In one case these weights were shifted as far as the pilot's seat. During the take-off runs the c.g. was at 26.0, 27.4, and 28.65 percent of the mean wing chord. The actual measurement was made under the same conditions and in the same way as that of the influence of the elevator deflection.

c) Measurement of the climbing speed with the c.g. in various positions.- Short climbs at full throttle and various dynamic pressures were made with the c.g. in different positions and only slightly changed total weight. The dynamic and air pressures were recorded. Measurements at 100 to 200 m height, with sufficiently constant dynamic pressure and under weather conditions with no vertical thermal air

currents at the flight altitude, were selected for subsequent interpretation. The results are plotted in figures 5 and 6. The fore-and-aft inclination was determined in several of these climbs (fig. 7).

d) Measurement of elevator deflections and control forces with the c.g. in various positions.— The elevator deflections and the corresponding stick forces were plotted in uniform flight at full throttle with the c.g. in six different positions. The stabilizer was fixed.

4. Interpretation of Measurements

a) Influence of elevator setting on the take-off.— The take-off run was determined as a function of the time plotted on a logarithmic scale and the exponent of the function of the take-off process $S = at^n$ was also determined. The speed was found by differentiating this function according to the time, and the take-off speed was determined by introducing the instant of pull-up into the resulting equation. With known wing loading, the take-off pressure and the lift coefficient at the moment of take-off could be approximately determined from this speed.

b) Relation between take-off and location of the c.g.— The interpretation of the measurements depends on the determination of the influence of the elevator setting. The take-off distance was again determined as a function of the time, speed, and lift coefficient at the moment of taking off.

c) Polars at full throttle.— The result of the climb measurement was used for calculating the polars at full throttle. Inasmuch as the climbing characteristics vary with the location of the c.g. a specific polar was found for each position of the c.g. The drag coefficient could not, however, be determined in absolute values, the engine power, the propeller efficiency and its variation with the coefficient of propeller advance not being known. Besides, the absolute values are not needed for comparing the polars at different locations of the c.g.

The engine power used in the calculation and its relation to the revolution number are shown in fig. 8. The variation of the propeller efficiency as a function of the

coefficient of propeller advance, based on earlier propeller tests, is plotted in figure 9.

d) Calculation of the angle of attack.— The angle of attack of the airplane was calculated from the angle of climb $\sin \varphi = v_{st}/v$ and the fore-and-aft inclination β .

e) Determination of the static stability with locked control.— The elevator deflections, measured for various locations of the c.g. as functions of the dynamic pressure, are plotted in figure 10 against the lift coefficients determined from the wing loading and dynamic pressure. These curves are straight lines with different gradients according to the location of the c.g. Their extensions cut the abscissa in a point corresponding to an elevator deflection of -13.2° (figure 11). The gradient of the elevator-deflection curves, expressed by $\partial \beta_H / \partial c_a$, was determined.

The moment coefficient $c_{mH} = M_H / q F t_m$ was determined for constant elevator settings and various dynamic pressures and positions of the c.g. This coefficient is plotted in figure 12 against the lift coefficient c_a . The gradient of the moment coefficient against the lift coefficient, namely $\partial c_{mH} / \partial c_a$, is a criterion for the stability with locked control.

The "static elevator effect" $\frac{d c_{mH}}{d \beta_H}$ may be derived from $\frac{\partial \beta_H}{\partial c_a}$ and $\frac{\partial c_{mH}}{\partial c_a}$. This effect, which in the present case is $\frac{d c_{mH}}{d \beta_H} = 0.0154$, is unaffected by the location of the c.g.

The static stability with locked control is usually expressed by $\frac{\partial c_{mH}}{\partial \alpha}$, which is the variation of the moment coefficient with the angle of attack. This value was determined.

f) Determination of elevator-control characteristics.— The stick force, which balances the control moments, was determined from test results at various fore-and-aft inclinations (fig. 2) and is plotted in figure 13 against the fore-and-aft inclination for various elevator settings.

For a further determination of the control characteristics the stick forces, measured in flight for a given location of the c.g., were plotted against the elevator

deflection. The fore-and-aft inclination corresponding in flight to each of the measured stick forces was also determined. The corresponding stick force produced by control moments was determined from the fore-and-aft inclination and elevator deflection in figure 13. Inasmuch as P equals $P_G + P_L$, the difference between the stick forces P measured in flight and the control forces P_G is the air force P_L exerted through the elevator on the control stick. P and P_G being negative in the measurement, positive values are obtained for P_L .

The elevator moment coefficient C_{RH} for each elevator setting was then determined from the following equation.

$$C_{RH} = \frac{P_L}{q F_{HR}} \times \frac{k_{eH}}{t_{HR}}$$

V. RESULTS OF THE INVESTIGATION

1. Flight Performances

a) Take-off.

Influence of elevator setting on the take-off distance.— After "pushing" the elevator control during the take-off run until the dynamic pressure required for hovering is reached, the airplane is taken off by pulling the control stick back. Under these conditions the take-off distance of the "Ente" is greater than if the elevator setting had been positive from the beginning. For an initial elevator deflection of -12.5° the take-off distance is 160 m (525 ft.), whereas, for an initial setting of 1° , it is only 130 m (426 ft.). The take-off speed of the airplane changes also. Thus, in the above example, it drops from 107 km/h to 89 km/h in accordance with the lift coefficients during take-off, which are $c_a \sim 0.7$ and $c_a \sim 1.1$ respectively (fig. 14).

These results are chiefly ascribable to the fact that the main landing gear lies far aft, as in the wind-tunnel model. The forward wing is therefore too heavily loaded on the ground. In future designs this influence will have to be overcome by mounting the main landing gear nearer to the c.g. of the airplane.

Influence of location of the c.g. on the take-off run.-
Variations in the location of the c.g. greatly affect the length of the take-off run. The latter is shortened by backward shifting of the c.g.

With the c.g. at -28.65 percent of the mean wing chord t_m , the take-off distance was approximately 200 m (656 ft.), whereas, with the c.g. at -26.0 percent of the t_m , this distance was only about 145 m (476 ft.). The take-off speed varied in the same proportion. It was 90 km/h in the first and 83 km/h in the second case. The lift coefficients at these speeds are $c_a \sim 0.98$ and $c_a \sim 1.16$ respectively. The test results are shown in figure 15.

Bad ground conditions increase the effect of the position of the c.g. on the take-off distance, since, with a constant total weight, the load on the front wheel increases with advancing c.g., pressing the wheels deeper into the soft soil. The influence of the location of the c.g. on the length of the take-off run is also explained by the rearward position of the main landing gear and can be reduced by mounting the landing gear nearer to the c.g. of the airplane.

b) Climbing speed.-

Influence of the location of the c.g. on the climbing speed.- As shown in figures 16 and 17, the climbing speed of the airplane varies, for the same total weight, with the position of the c.g. For a constant dynamic pressure the climbing speed decreases with advancing c.g. However, the measurements are extended to positions of the c.g. which lie beyond the admissible limits. These limits were exceeded in the direction of decreasing climbing speed. In practice, the airplane is never flown with the c.g. in the two foremost positions $r = -29.3$ and $r = -29.65$ percent of t_m at which the smallest climbing speeds were recorded.

As shown in figure 17, the dynamic pressure at maximum speed also changes with the position of the c.g. However, the same restriction applies to this case as to the climbing-speed measurement. The c.g. cannot exceed an admissible forward limit $r = -28.5$ per cent of t_m . With the c.g. in this position, the impact pressure at maximum speed is 86 kg/m². More advanced positions of the c.g., with smaller dynamic pressures at maximum speed, cannot occur in practice.

Climbing-speed measurements involve considerable sources of error. The engine power varies slightly on different days. The relation between the specific gravity of the air and the altitude is also subject to variation. The air is seldom free from vertical thermal air currents. The instruments, especially aneroid barometers, are subject to many errors and the clockworks are not fully proof against temperature variations. The present measurements required great caution. All records showing a material variation of the engine speed, temperature inversion, departures from the region between 100 and 200 m altitude, or turbulent weather conditions were discarded. The data remaining after exclusion of these doubtful items seemed sufficiently reliable for a determination of the order of magnitude of the climbing speed variations with the position of the c.g.

Observations made in a series of flights show that two different flight conditions may occur at very small and very large dynamic pressures. Thus, the climbing speed was very small when, taking off with fully deflected elevator, this deflection was gradually reduced. On the other hand, a greater climbing speed was reached when the elevator control was pushed well forward for a short time after the take-off and then pulled back again to the same dynamic pressure as above. Similar conditions prevailed at large dynamic pressures. At times downward vertical velocities up to 5 m/s were reached in flight at full throttle with dynamic pressures of approximately 120 kg/m², whereas, under normal conditions the downward vertical velocity at such pressures is only half the above value. These conditions are ascribable to changes in the form of flow about certain parts of the airplane. The changes are caused or affected by the magnitude, direction and rapidity of the elevator deflection and by variations in the initial direction of flow.

In estimating the influence of the location of the c.g. on the climbing speed and dynamic pressure at maximum speed allowance must be made for the fact that these measurements cover a range of c.g. positions considerably exceeding practical requirements.

Even the performances of airplanes with control surfaces at the rear vary with the position of the c.g., especially when the airplane is very stable about the transverse axis. The setting of the wing with respect to the

Horizontal tail surfaces (i.e. the longitudinal dihedral) must be increased with the static fore-and-aft stability. This results in a greater induced drag of the airplane.

For the same reason, an increase of the induced drag of the "Ente" is unavoidable with increasing static stability. The designer proved, however, that his increment is too small to account for the measured variation of the climbing speed with the position of the c.g. The observed variations of the climbing speed seem to be due to separation of the flow from the lower surface of the main wing, caused by variations of the downwash and, on the upper surface of the forward wing, by the fuselage. Similar separation phenomena, repeatedly observed in wind-tunnel tests, are accompanied by a marked increase in the profile drag. According to this explanation the observed variation of the climbing speed is not inherent in tail-first types, but merely an incidental aerodynamic defect of the present example.

Influence of the location of the c.g. on the flight polars.— The influence of the location of the c.g. is also shown by the comparative polars in figure 18. The measured drag coefficient increases with forward shifting of the airplane c.g. The angles of attack are marked in the comparative polars of figure 18. As shown in figure 19, the absolute values of these angles change with the location of the c.g. The increase of the lift coefficient with the angle of attack $\partial c_L / \partial \alpha$, shown in figure 20, also depends on the location of the c.g.

The above explanations for the variation of the climbing speed also apply to the drag variation. The latter is chiefly attributable to the influence of incidental separation phenomena not inherent in the tail-first type.

2. Flight Characteristics

a) Taxiing characteristics.— Wheel brakes and throttle control of the two engines afford excellent maneuverability on the ground. Inasmuch as this airplane cannot capsize, the taxiing speed and the brake force are not limited by the elevator setting.

b) Take-off and landing characteristics.— According to the above measurements, the best take-off conditions are

reached by pulling the elevator control back from the beginning of the run. The forward wing rises first, followed shortly by the airplane, which oscillates simultaneously about the transverse axis. After the take-off the best practice is to "push" the elevator control well forward for a moment. Otherwise, the lift is deficient probably on account of separation of the flow from the forward wing. This short "push" apparently causes the flow to conform and the climb again becomes normal. In general, this airplane can be taken off very easily.

The initial landing maneuver is identical with that of airplanes of orthodox design. The estimation of the height above the ground, required for flattening out, is greatly facilitated by good visibility. Upon approaching the ground, the elevator control is pulled slowly back until the rear wheels touch the ground. If the elevator remains "pulled" during the landing run, the front wing drops with a jerk, probably on account of the far backward position of the main landing gear. It is therefore advisable to push the control stick slowly forward, after the rear wheels touch the ground. The front wheels then come down smoothly and gradually. The landing maneuvers are extremely simple and "bad landings" are practically impossible.

c) Stability characteristics.

Stability with locked control and controllability about the transverse axis.— Static stability with locked control is denoted by $\partial c_{mH} / \partial c_a$. This expression is a linear function of the location of the c.g. (fig. 21). With the c.g. in the foremost of the investigated positions, at -29.65 percent of the mean wing chord, the stability was $\frac{\partial c_{mH}}{\partial c_a} = 0.135$. With the c.g. in the rearmost position, at -26 percent of the mean wing chord, this value was $\frac{\partial c_{mH}}{\partial c_a} = 0.096$. Under normal load conditions, the stability with locked control is approximately of the same magnitude as that of the Junkers F 13 ge. The location of the c.g., when the stability is nil, can be determined by extrapolation. The point of "neutral equilibrium" is at -16.3 percent of the mean wing chord.

In the case of tail-first airplanes, stability cannot be expressed by $\partial c_{mH} / \partial \alpha$, at least not for comparing

stabilities with the c.g. in different positions (fig. 22). Inasmuch as $\partial c_a / \partial \alpha$ changes with the shifting of the c.g., the variation of the moment coefficient with the angle of attack is not a reliable standard of comparison. On the contrary, considering the relation between lift and angle of attack, the aerodynamic condition of the tail unit differs for each position of the c.g.

The static elevator effect $d c_{mH} / d \beta_H$ is obtained from $\partial c_{mH} / \partial c_a$, which denotes the static stability, and $\partial \beta_H / \partial c_a$, indicating the variation of the elevator setting with the lift coefficient. The static elevator effect, which equals 0.0154, is unaffected by the location of the c.g. For Junkers F 13 airplanes flying at full throttle this figure is 0.020. The stability figures determined in flight agree well as to magnitude with those obtained by wind-tunnel measurements. While the flight figures $\partial c_{mH} / \partial c_a$ are invariable within the range of practical lift values, for each position of the c.g. and all lift coefficients, the wind-tunnel figures vary slightly with the lift.

Stability with released control and elevator-control characteristics.— The results of the control-force measurements in figure 23 show considerable scattering. This is chiefly due to the insufficient accuracy of only ± 100 g of the DVL control-force recording device and to the influence of control friction which was large, as compared with the small absolute values, and reduced the control forces in uniform flight. On the bench, the friction measured at the control stick was 1.2 to 1.6 kg (2.6 to 3.5 lb.). In flight the control friction decreased materially as a result of vibrations in the bearings and transmission pulleys. The remaining friction increased the dispersion of the points of measurement. The manual forces measured in flight were less than 1 kg. The variation of the manual forces with the dynamic pressure was not linear, nor the gradient of the manual force above the dynamic pressure, plotted against the location of the c.g., uniformly straight as for all previously tested airplanes. The smallness of the measured forces was chiefly due to the small elevator chord and the rearward location of the elevator axis.

The relation between the elevator moment coefficient c_{RH} and the elevator deflection (fig. 26) likewise depends

on the angle of attack.* Yet the curve of the elevator moment coefficient permits of an approximate estimation of the elevator balance. The elevator moment coefficient is small between -9° and -7° . Its increase is linear from -7° to -4° . This curve agrees with the results of Göttingen wind-tunnel measurements with similar tail-surface sections (reference 1).

As mentioned above, the variation of the manual forces in flight is not linear with the dynamic pressure. It is curvilinear, and intersections with the abscissa occur for two different dynamic pressures (fig. 23). These intersections, coincident with zero manual force, correspond to equilibrium with released control. Thus equilibrium with released control is achieved in each case for two different dynamic pressures. The sign of stability with released control shows the sign of the gradient of the manual forces above the dynamic pressure $\partial P / \partial q$. According to the curve of the manual forces, the airplane is stable with released control at small dynamic pressures and unstable at large dynamic pressures.

This statement is based on figure 24 in which the stick forces are plotted against the elevator setting, the c.g. being in a position in which the dispersion of the points of measurement is relatively small. The figure shows that the negative force P_G , produced by the moments of the control weight, including the weight of the elevator, is greater than the manual force measured in flight. The manual and control forces have, however, the same direction. The difference between the two forces is P_L , the air force moment on the control stick. Its sign is therefore opposite to the sign of the manual force in flight and to that of the control force.

The direction of the control moments of airplanes with rearward control surfaces is exactly opposite. In normal flight the main part of the control moments usually consists of the unbalanced moment of the elevator weight. The elevator drops in normal flight and on the ground. In airplanes with rearward tail unit this drop results in an elevator deflection corresponding to a reduction of the angle of at-

*In order to determine the true relation between the elevator moment coefficient and the elevator setting, tests with different stabilizer settings would have to be made. This, however, was impossible, since the stabilizer was not adjustable.

tack. The elevator of the tail-first type also drops, but in forward tail units the resulting elevator deflection corresponds to an increase in the angle of attack. In both types, the moments of the elevator weight have the same direction about the elevator axis, but are opposite with respect to the airplane. In the tail-first airplane the direction of the elevator weight moments with respect to the airplane does not, as in most standard airplane types, increase stability with released control over stability with locked control (reference 2).

A slight modification easily permits reversing the direction of the elevator-force moments on finished airplanes. Weight balances must be fitted forward of the elevator hinge. This change brings the elevator forces in a linear relation to the dynamic pressure, thus extending stability with released control to the whole range of dynamic pressures. Besides, stability with released control is thus materially increased and extended to positions of the c.g. at which the airplane is usually unstable with locked control. The result of the proposed modifications is shown numerically in figure 25.

Stability about the vertical and longitudinal axes. This stability has not yet been measured. A qualitative estimate shows a small degree of stability about the longitudinal axis and considerable stability about the vertical axis. Special tests are planned to study stability about the vertical axis and the influence of the ailerons. Accurate measurements of lateral airplane stability for various lift coefficients are also planned.

d) Behavior at large angles of attack.- When the elevator control is pulled back and held in this position in straight flight, the nose of the airplane rises to a large positive fore-and-aft inclination and then drops back gradually and without jerks. After reaching a slight negative fore-and-aft inclination the airplane flattens out again and the process is repeated. The flight path with pulled elevator is an oscillation of apparently constant frequency and amplitude in a vertical plane. A study of this motion is planned. When the rudder is gradually deflected with pulled elevator control, the airplane makes a spiral with negative fore-and-aft inclination. No tests were made with jerky elevator deflections at large angles of attack for investigating the spinning characteristics of the airplane. Such tests may be fatal to both airplane and pilot, since

the latter can hardly leave the airplane with a parachute due to the relative position of the propellers and the pilot's seat.

e) Flight in squalls.- In squalls the minimum dynamic pressures were not always as small as in still weather. In squalls the airplane nosed down at relatively great dynamic pressures. Apparently turbulent air promotes the separation of the flow from the forward wing.

The airplane motion about the transverse axis is particularly remarkable in squalls. While the oscillations of the airplane about the other axes, under the action of squalls, are normal, those about the transverse axis, even for slight disturbances, are considerable. In order to eliminate the influence due to the operation of the controls the elevator was held in exactly the same position without deflection. Even with constant elevator setting, the oscillations of the airplane about the transverse axis remained unchanged. It was first thought that this observation was due to an error made by the pilot, on account of the unusual position of the axis of rotation and of the pilot's seat with respect to this axis. The airplane was therefore observed from the ground to obviate possible errors. Its motions were thus compared with another simultaneously observed airplane of standard design. The oscillations about the transverse axis, due to squalls, were clearly visible from the ground. The standard airplane with rearward control surfaces did not visibly oscillate about the transverse axis.

The behavior of the airplane in squally weather is due to the fact that, for the existing elevator deflection, the forward wing is near its maximum lift. Ascending gusts cause separation of the flow from the forward wing. This separation causes the airplane to nose down until the flow conforms again. This explanation is confirmed by the above remark that the minimum speed in squalls is smaller than in quiet weather, the flow about the forward wing tending to cause separation in squalls.

f) General behavior in flight.- In spite of a normal static elevator effect, the airplane seems to be unusually responsive to elevator deflections. This impression of great dynamic control efficiency is due, in part, to the relatively small elevator forces, as compared with the aileron and rudder forces.

The airplane can be side-slipped in spite of its great directional stability. With one engine stopped, the airplane can be flown straight and in curves, but loses altitude. In quiet weather and under normal flight conditions this type behaves exactly like up-to-date airplanes with rearward control surfaces.

g) Trial flights.— In the winter of 1931 the designers of the airplane made a great number of cross-country flights to Zurich, Copenhagen, London, etc. A total distance of 6,000 km was flown. The airplane proved satisfactory even in bad weather, thus showing its reliability and practical utility.

VI. SUMMARY OF RESULTS

1. Flight Performances

The length of the take-off run depends on the elevator setting and on the location of the c.g. This seems to be due to the rearward position of the main landing gear, adopted in conformity with model tests. This feature may be improved in future airplanes.

The climbing speed and the dynamic pressure at the maximum speed vary with the location of the center of gravity. These variations are probably due chiefly to accidental separation phenomena which can be avoided in future designs.

2. Flight Characteristics

Maneuverability on the ground is very good, without danger of capsizing. Take-off and landing maneuvers are extremely simple.

Static stability with locked controls is about the same as that of the Junkers F 13 ge airplanes. The static elevator effect has the same magnitude as that of standard airplanes.

Stability is smaller with released than with locked controls, the direction of the control moments, with respect to the airplane, being opposite to that of the moments

on airplanes with rearward control surfaces. This difficulty can be easily obviated, even on the existing type, by means of balance weights.

The airplane has small lateral stability but comparatively great directional stability. Quantitative tests have not yet been made.

As intended by the designer, the airplane recovers from stalls by gradually modifying its flight path and automatically returning to small angles of attack. The altitude lost in recovering from stalls will be measured later. This loss is a criterion of the improved safety in stalls.

In squalls the airplane has a tendency to oscillate about its transverse axis. This feature is ascribable to separation of the flow, avoidable in future designs.

The airplane seems to be unusually responsive to elevator deflections. This impression is given by the very small elevator forces as compared with the aileron and rudder forces.

The airplane can be side-slipped in spite of its great directional stability. With one engine stopped, the airplane can be flown straight and in curves, but loses altitude.

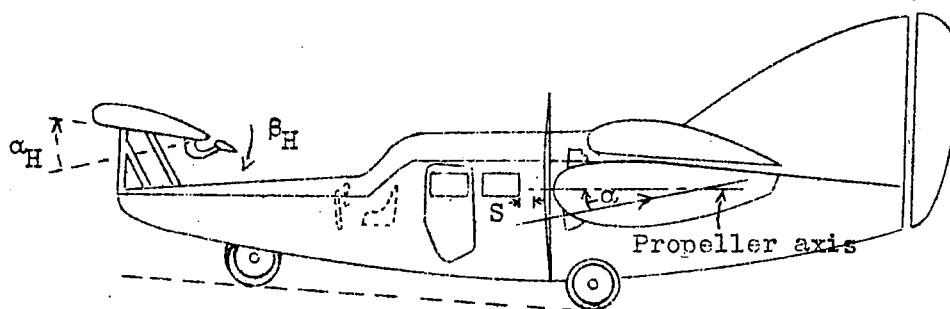
In quiet weather and under normal flight conditions this airplane flies like up-to-date types with rearward control surfaces.

In flights made by the designers over a distance of 8,000 km, the airplane proved its reliability and practical usefulness, even under very unfavorable weather conditions.

Translation by W. L. Kaporindé, Paris Office,
National Advisory Committee for Aeronautics.

REFERENCES

1. Prandtl, L.: Effect of Streamline Curvature on Lift of Biplanes. T.M. No. 416, N.A.C.A., 1927.
2. Blenk, Hermann: Ueber die Längsstabilität eines Flugzeuges mit losgelassenem Höhensteuer. ZfM, vol. 21, no. 8, 1930, p. 189, and DVL-Yearbook, 1930, p. 61.



Total wing area	$F = 35.7 \text{ m}^2$	284 sq. ft.
Area of forward wing	$F_H = 6.2 \text{ "}$	66.7 "
Area of elevator	$F_{HR} = 1.7 \text{ "}$	18.3 "
Span of main wing	$b_{HR} = 14.0 \text{ m}$	45.9 ft.
Span of forward wing	$b_H = 5.2 \text{ m}$	17.0 ft.
Elevator chord	$t_{HR} = 0.3 \text{ m}$	0.98 "
Weight empty, equipped	$G_R = 1175 \text{ kg}$	2590 lb.
Total weight during tests	$G = 1500 \text{ to } 1575 \text{ kg}$	3307 to 3472 lb.
Acceptance weight	$G_{\max} = 1650 \text{ kg}$	3628 lb.
Range of c.g. in tests	-26.0 to -29.65 % of t_m	
Acceptance range of c.g.	-23.2 to -28.5 % t_m	
Mean wing chord t_m	2.5 m	3.2 ft.
Distance between leading edge at mean wing chord and at fuselage	0.08 m	3.1 in.
Angle of forward wing setting with respect to center of main wing, approximately 10° .		

Figure 1.-Side view of the Focke-Wulf F 19a "Ente" airplane.

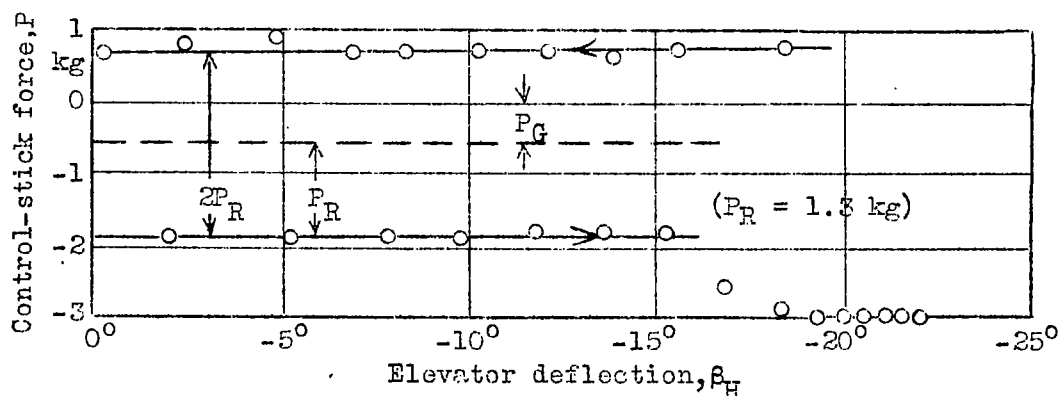


Figure 2.-Friction and control force on control stick with fore-and-aft inclination of 8.1° . In normal flight the friction force is not affected by the elevator setting. It is 1.2 to 1.6 kg (2.6 to 3.5 lb.) at the stick. In flight, friction is reduced by vibration.

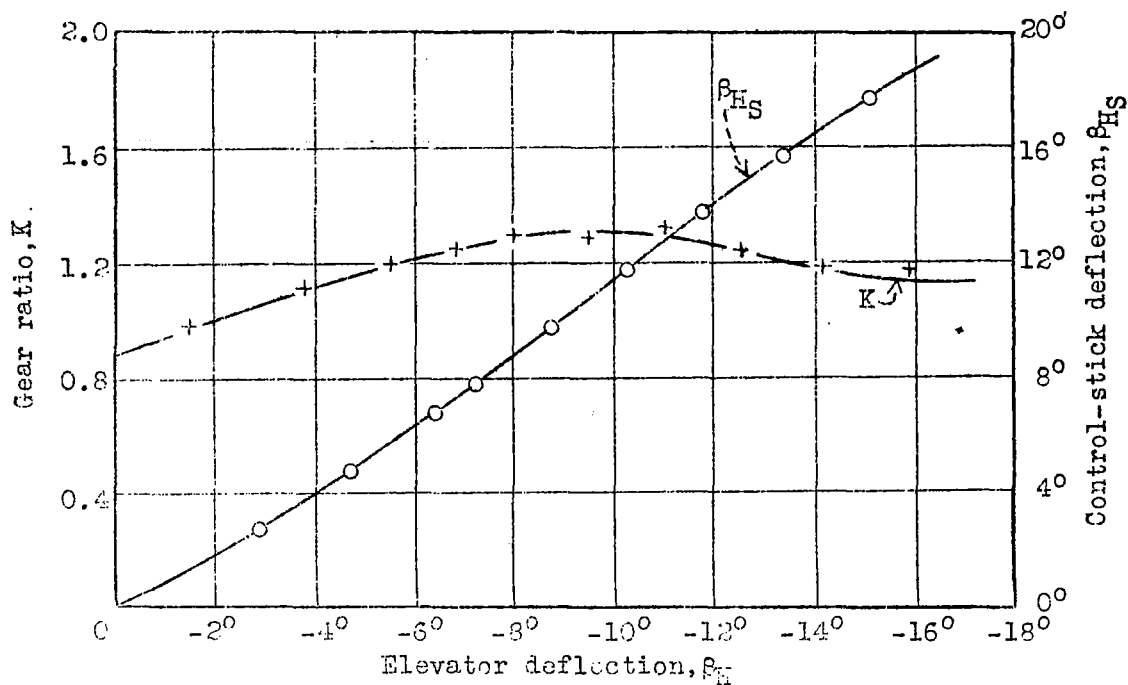


Figure 3.-Elevator control gear. The gear ratio changes with the elevator setting.

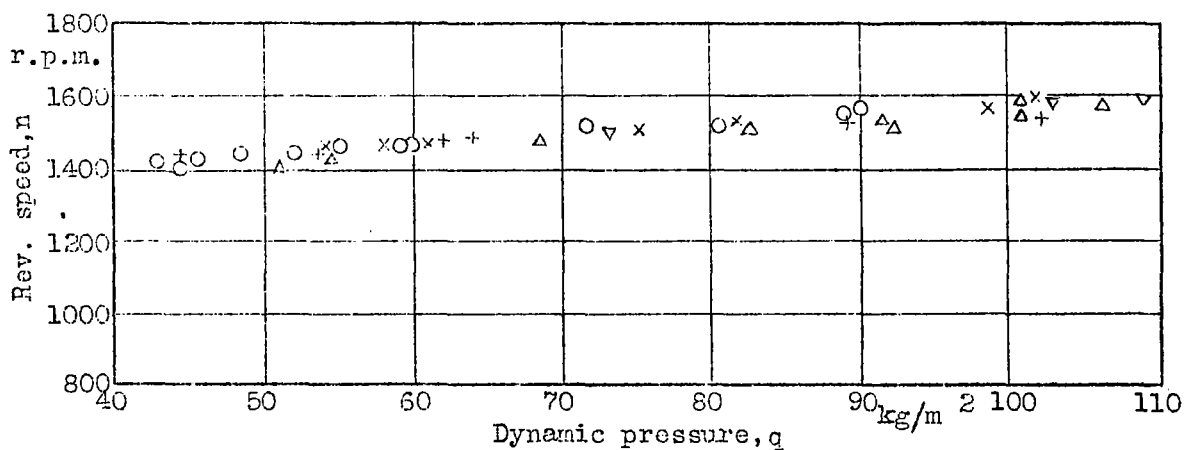


Figure 4.-Calibration of Heine propellers 50900 and 50901. Pitch 2.11 m (6.9 ft.), diameter 2.45 m (8.0 ft.). The various points of the diagram were plotted in different flights.

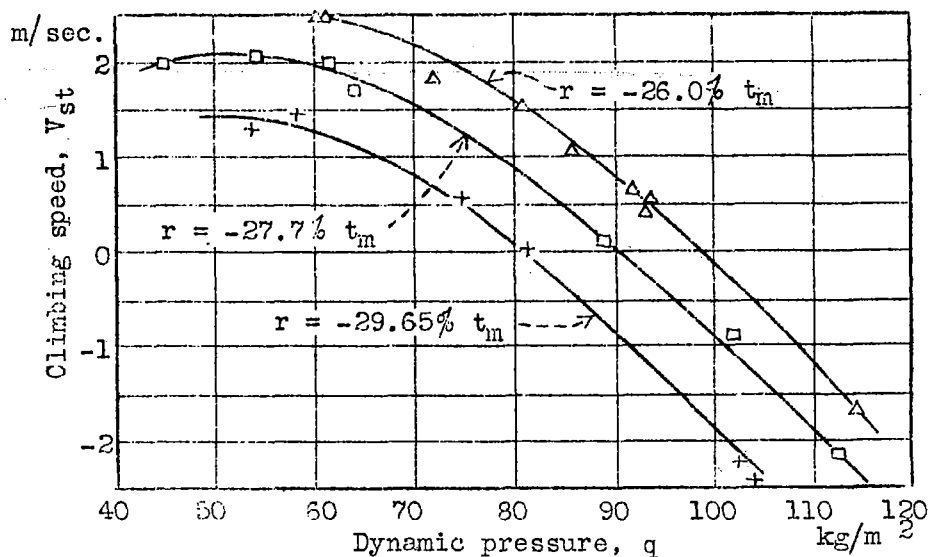


Figure 5.-Climbing speed with c.g. at -26.0, -27.7, and -29.65% of the mean wing chord. The airplane weight differed in each test flight. The c.g. at -29.65% of t_m is outside the acceptance limits.

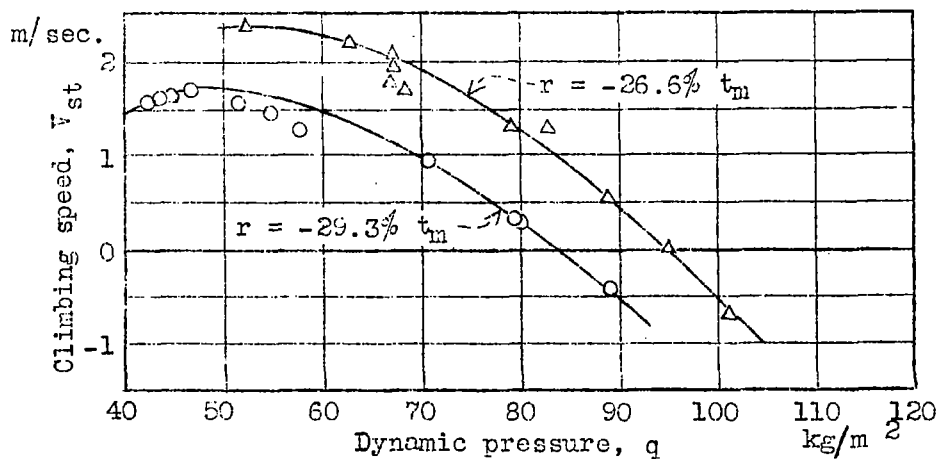


Figure 6.-Climbing speed with c.g. at -26.6 and -29.3% of the mean wing chord. The c.g. at -29.3% of t_m lies outside the acceptance limits.

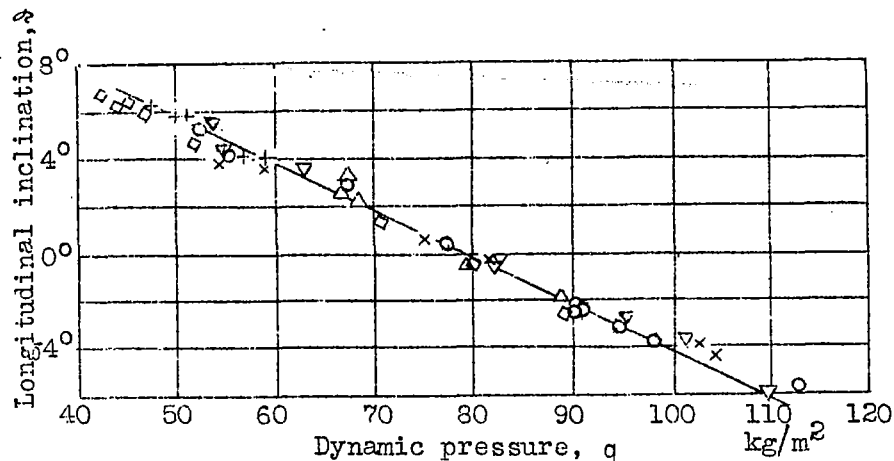


Figure 7.-Fore-and-aft inclination vs. dynamic pressure. The fore-and-aft inclination was plotted with a pendulum. Different marks are used to denote points found in different flights.

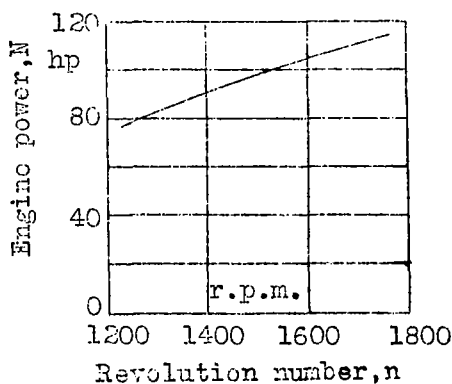


Figure 8.-Assumed relation between full power and revolution number of Siemens SH 14 engines. Relation between power N and revolution number n was determined on the torque stand.

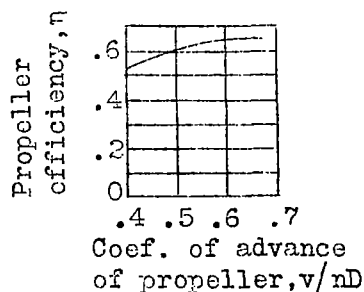


Figure 9.-Assumed efficiency curve of Heine 50900 and 50901 propellers. Relation between the efficiency and coefficient of advance was assumed on basis of measurements with propellers of similar pitch ratio.

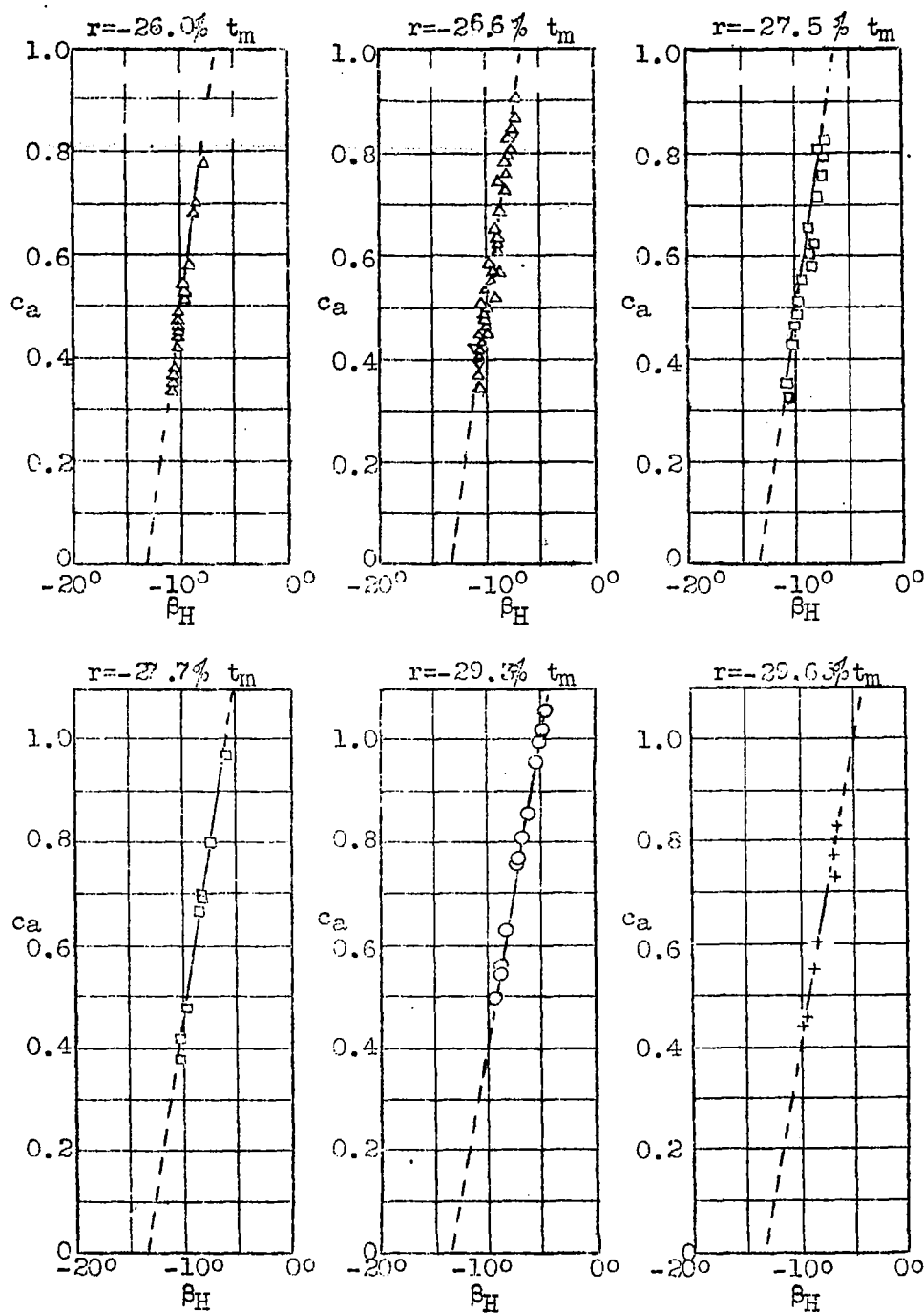


Figure 10.—Relation between lift coefficient and elevator setting with c.g. in various positions. The relation between lift coefficient and elevator deflection is approximately linear for each location of the c.g.

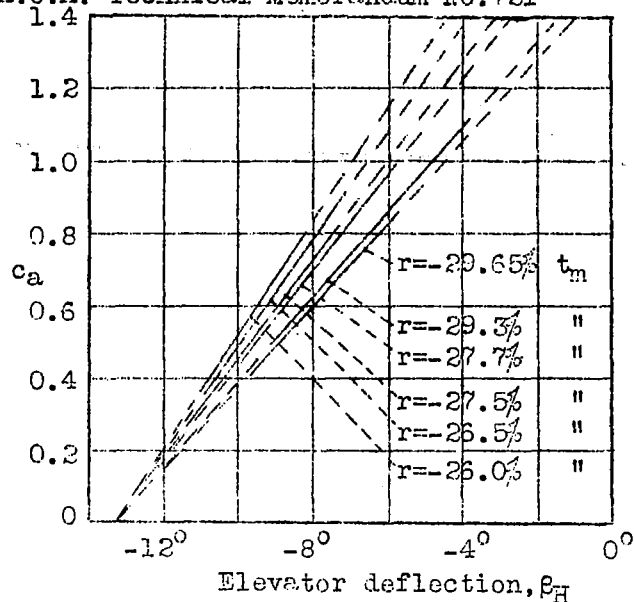


Figure 11.-Relation between lift coefficient and elevator deflection for various locations of the c.g. Gradient of elevator deflection curves varies with the location of the c.g. The curves intersect near $c_a = 0$.

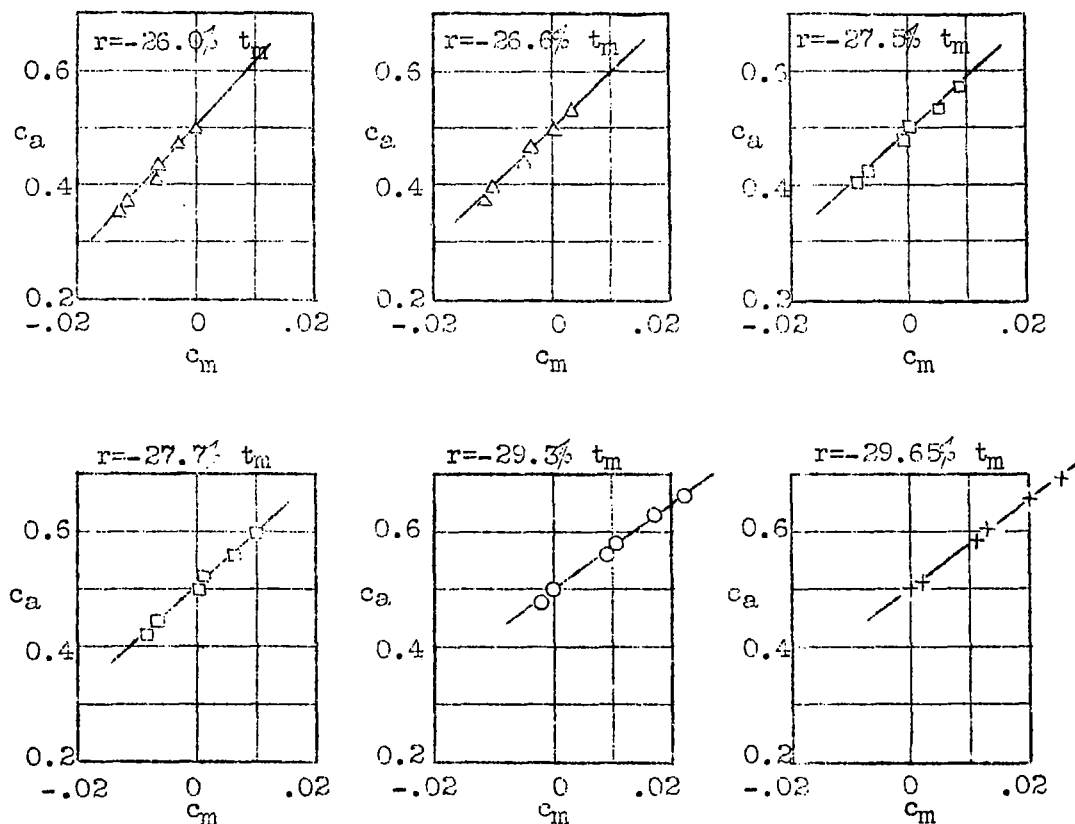


Figure 12.-Lift coefficient against moment coefficient for various positions of the c.g. Gradient of moment curve changes with location of the c.g.

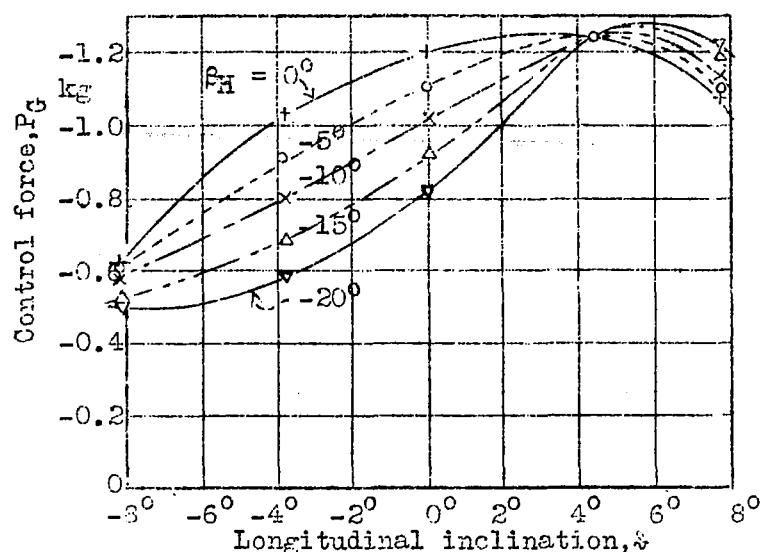


Figure 13.-Control force on control stick against fore-and-aft inclination β and elevator deflection β_H . Force exerted on control stick by moments of control weights depends on elevator setting and fore-and-aft inclination. Direction of variation of force with elevator deflection is opposite to that of airplanes with horizontal tail surfaces at the rear.

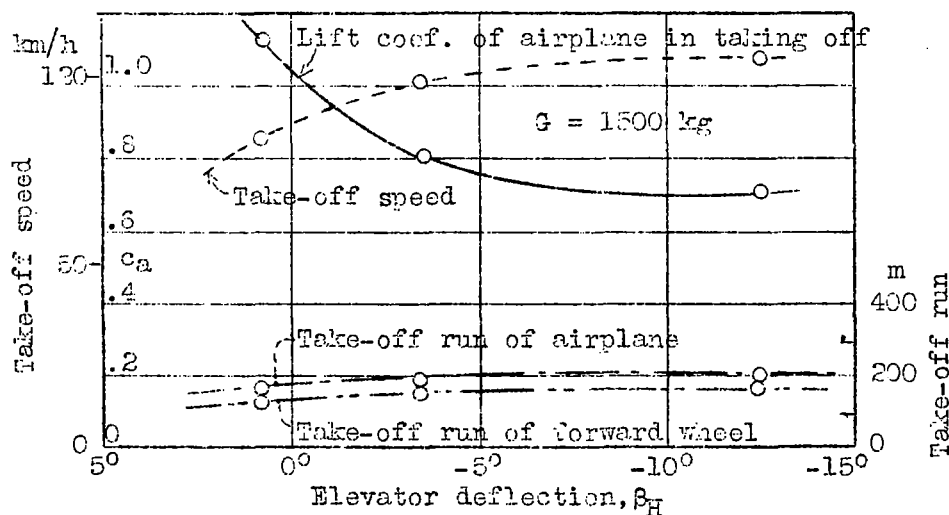


Figure 14.-Influence of elevator deflection on take-off. Take-off run and speed increase with forward pushing of elevator control at beginning of take-off.

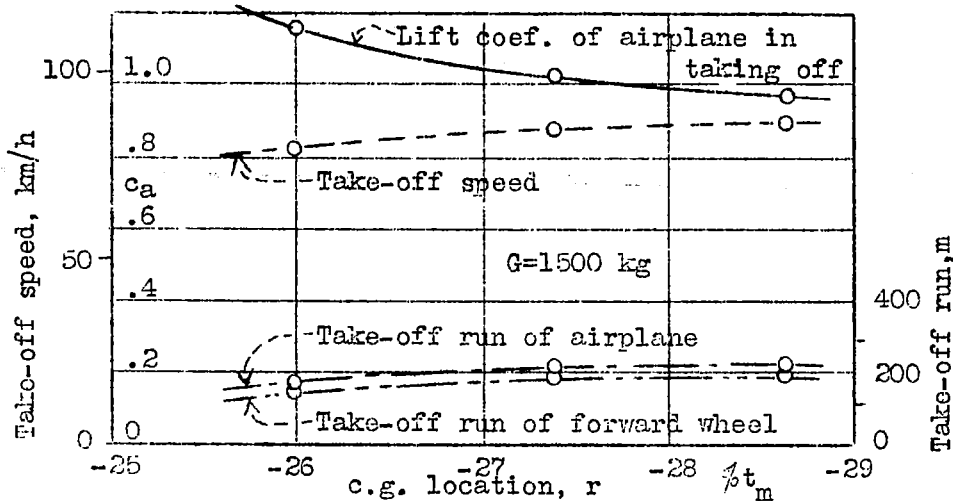


Figure 15.-Relation between the position of the c.g. and the take-off. A forward shifting of the airplane c.g. increases the take-off run and speed.

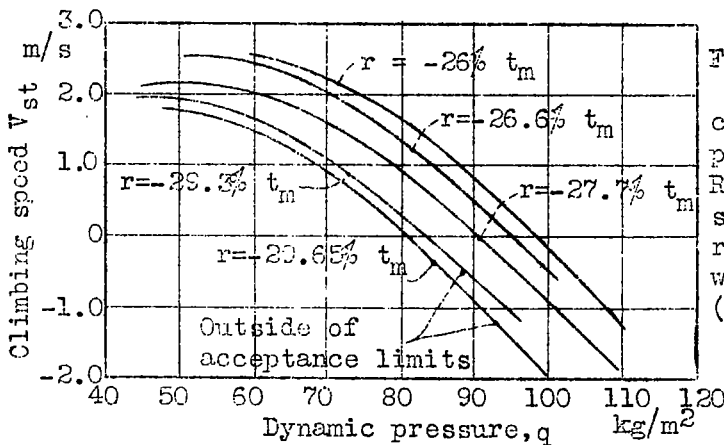


Figure 16.-Climbing speeds with c.g. in different positions ($G=1500$ kg). Results of climbing-speed measurements are reduced to same total weight $G=1500$ kg (3307 lb.)

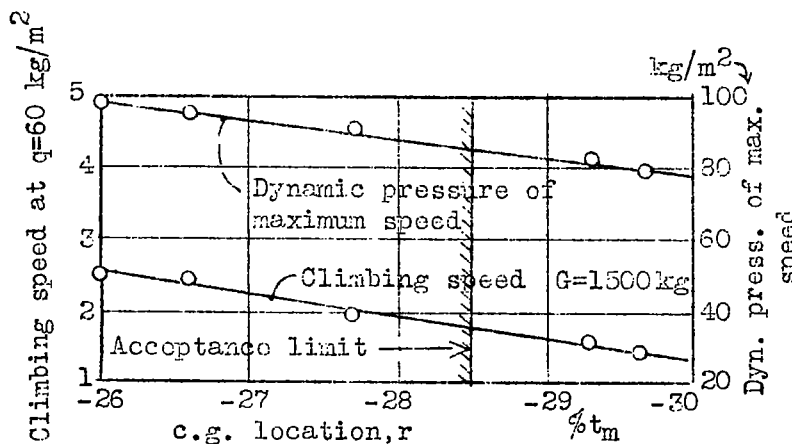


Figure 17.-Variation of climbing speed and dynamic pressure at maximum speed according to position of c.g. Forward shifting of c.g. reduces climbing speed and dynamic pressure at maximum speed. This variation is small within acceptance limits.

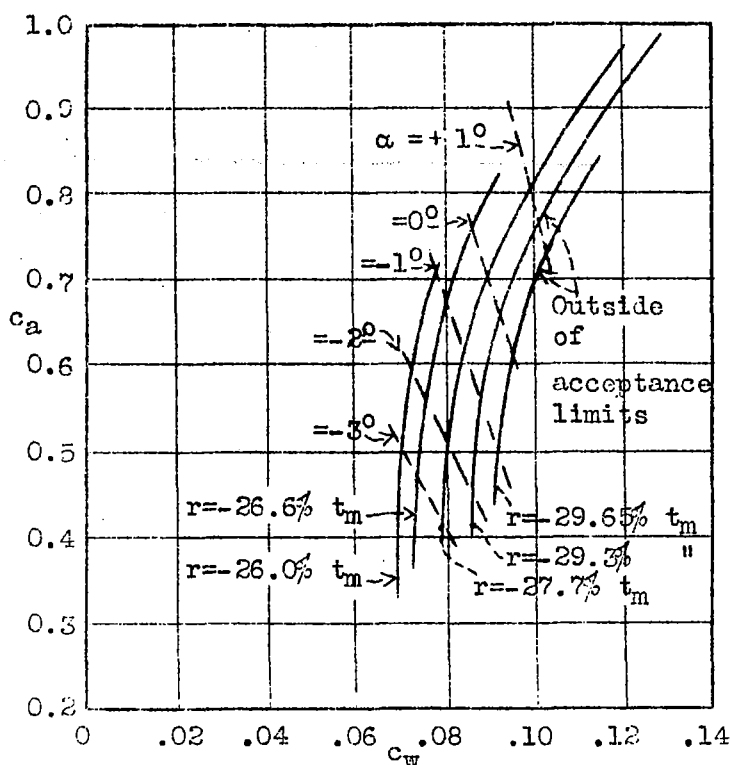


Figure 18.-Full-throttle polars with c.g. in different positions. Flight polars with c.g. in different positions were determined from climbing-speed measurements based on assumptions of figs.8 and 9. The increase in drag, resulting from a forward shifting of the c.g., is due to incidental separation of the flow.

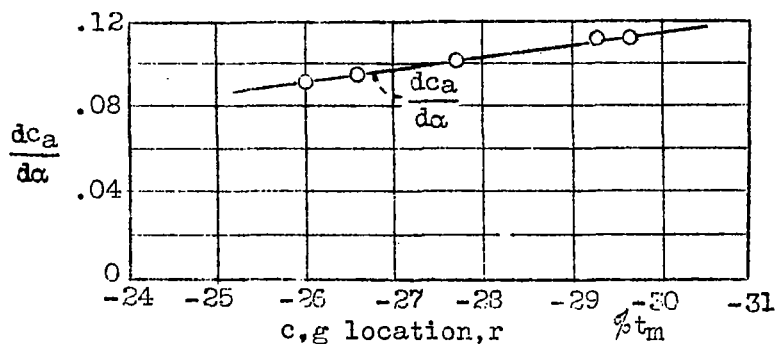


Figure 20.-Relation between $dc_a/d\alpha$ and location of c.g. Gradient of lift to angle of attack increases with forward shifting of c.g.

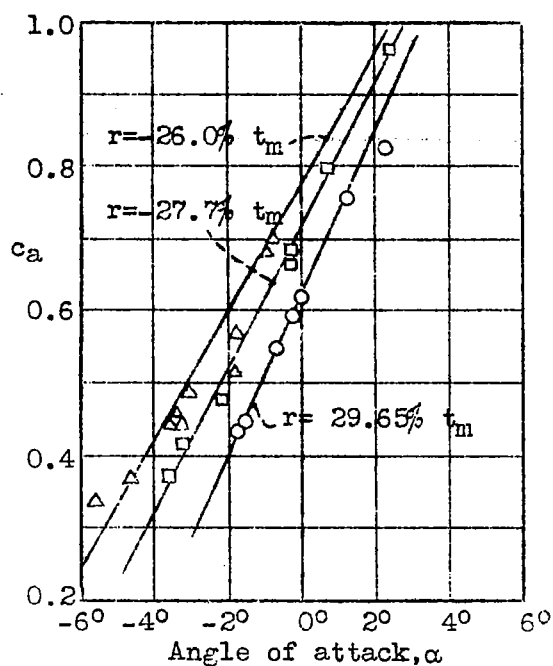
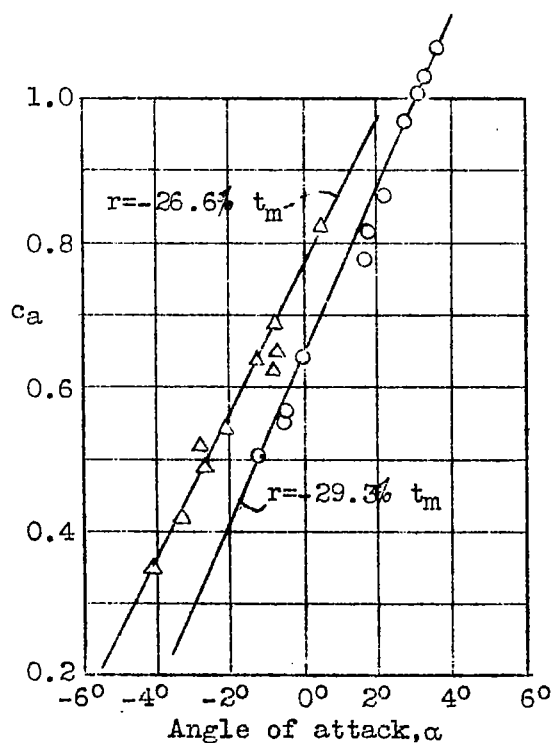


Figure 19.-Lift coefficient against angle of attack with c.g. in various positions. Relation between lift coefficient and angle of attack changes with location of c.g.



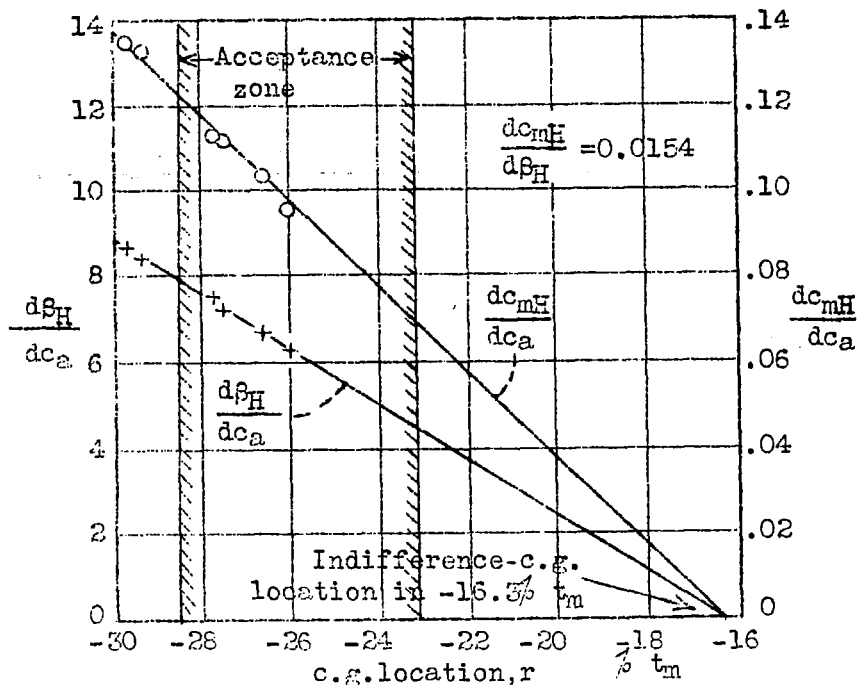


Figure 21. $\frac{dc_{mH}}{dc_a}$ and $\frac{d\beta_H}{dc_a}$ against location of c.g. The static stability

$\frac{dc_{mH}}{dc_a}$ and the static elevator effect $\frac{d\beta_H}{dc_a}$ are of the same order of magnitude as those of good airplane types with rearward control surfaces. Thus the $\frac{dc_{mH}}{dc_a}$ of the Junkers F 13 ge is approximately 0.06 and $\frac{dc_{mH}}{d\beta_H} \sim 0.02$. With the c.g. at $-16.3\% t_m$ the airplane is in statically neutral equilibrium about the transverse axis $\frac{dc_{mH}}{dc_a} = 0$.

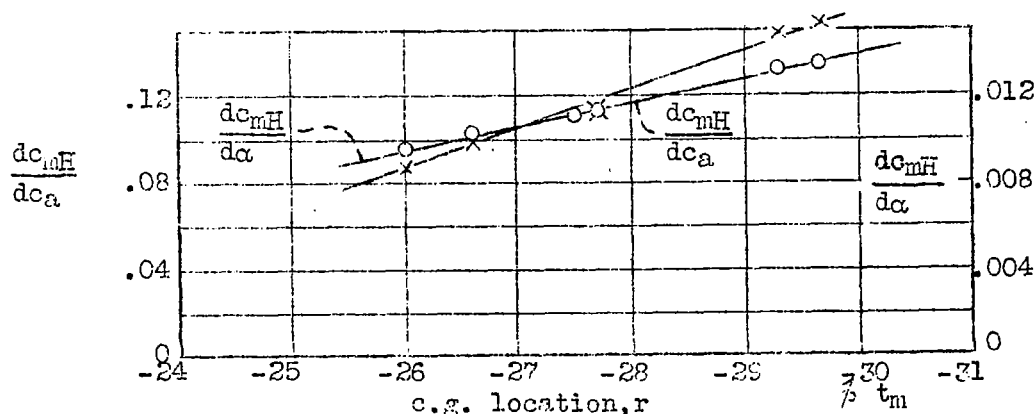


Figure 22. $\frac{dc_{mH}}{d\alpha}$ and $\frac{dc_{mH}}{dc_a}$ plotted against location of c.g.

Inasmuch as $\frac{dc_a}{d\alpha}$ changes with the position of c.g., $\frac{dc_{mH}}{dc_a}$ and $\frac{dc_{mH}}{d\alpha}$ stand in different relations to the position of the c.g.

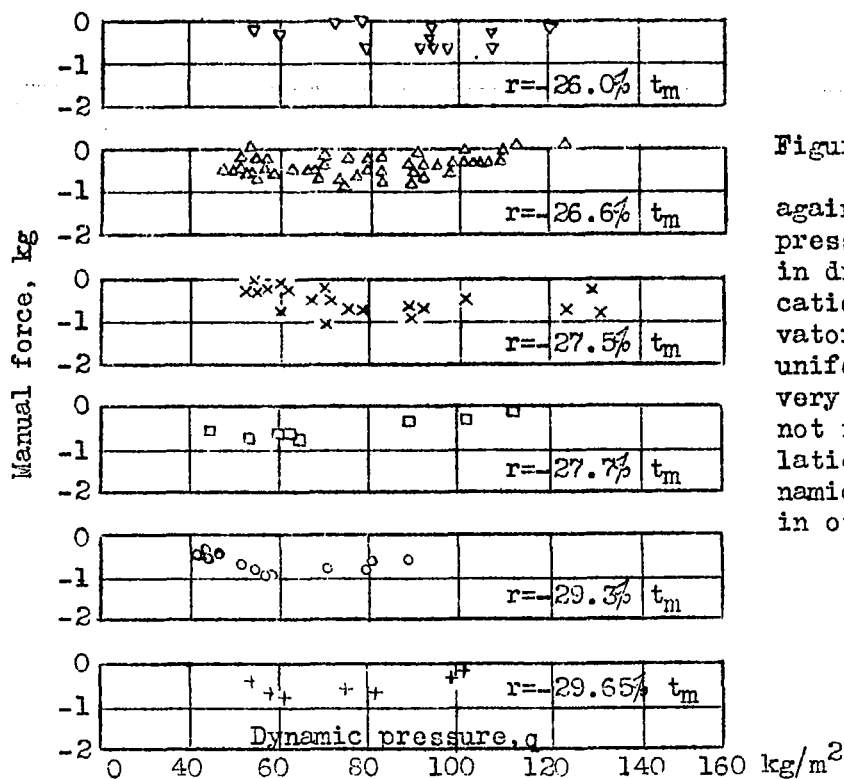


Figure 23.-Control force against dynamic pressure with c.g. in different locations. The elevator forces in uniform flight are very small and are not in a linear relation to the dynamic pressure, as in other airplanes.

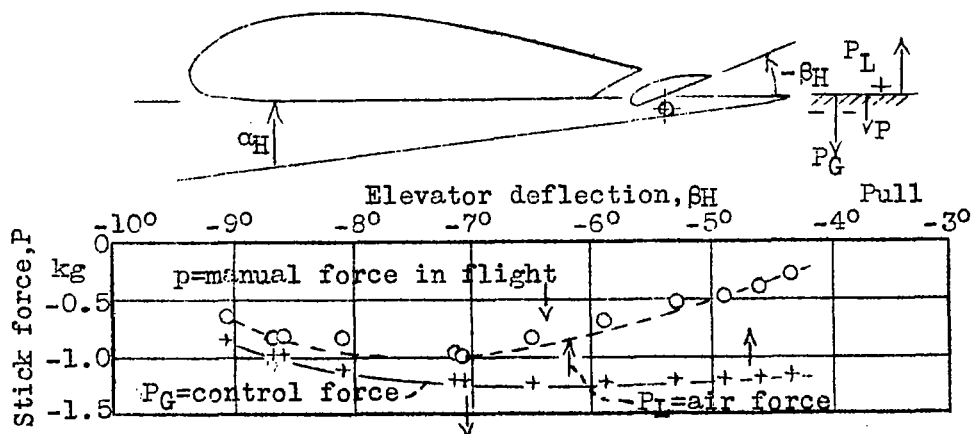


Figure 24.-Stick forces against elevator setting. c.g. at -29.3% of t_m.

Negative force P_G , which is produced by the moments of the control weight including that of the elevator, is greater than the manual force measured in flight. The difference between the manual and control forces is force P_L on the stick, exerted by the air-force moments about the elevator axis. This force has an opposite sign to that of the manual force in flight.

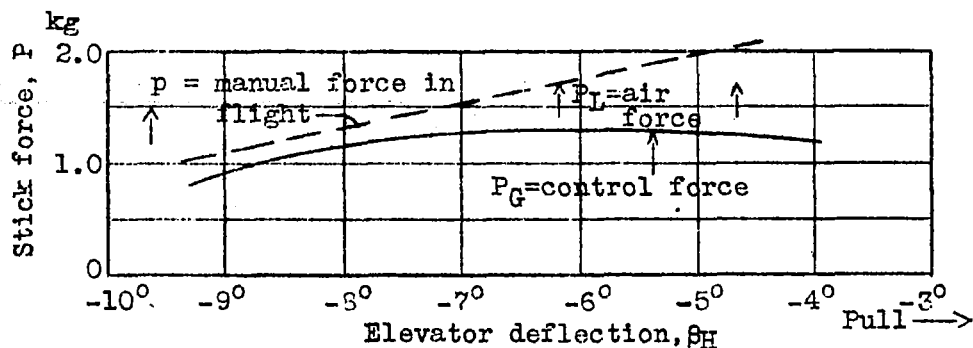


Figure 25.-Proposed modification of manual force gradient by changing sign of control force (use of balance weights). The sign of the control force P_G is changed by balance weights forward of elevator axis. This change establishes a linear relation between the manual force in flight and the elevator deflection, as in other airplane types, thus increasing the stability with released control.

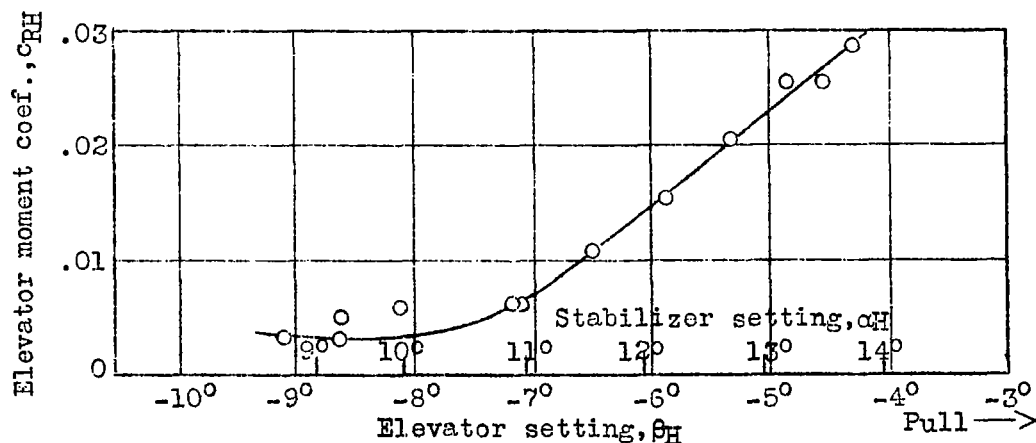


Figure 26.-Elevator moment coefficient against elevator setting with the c.g. at $-29.3\frac{1}{2} t_m$. This curve also allows for influence of angle of attack. The elevator moment coefficient is small between $\beta_H = -9^\circ$ and -7° . It increases linearly from $\beta_H = -7^\circ$ to -4° . This agrees with the results of wind-tunnel measurements with similar control surfaces.